A&A manuscript no.
(will be inserted by hand later)

Your thesaurus codes are:
02(09.04.1; 11.09.3; 12.04.1)

ASTRONOMY AND ASTROPHYSICS

Can Dust Segregation Mimic a Cosmological Constant?

Jakob T. Simonsen and Steen Hannestad

Institute of Physics and Astronomy, University of Aarhus, DK-8000 Århus C, Denmark

February 1, 2008

Abstract. Recent measurements of type Ia supernovae indicate that distant supernovae are substantially fainter than expected from the standard flat cold dark matter model. One possible explanation is that the energy density in our universe is in fact dominated by a cosmological constant. Another possible solution is that there are large amounts of grey dust in the intergalactic medium. Dust grains can be grey either because they are non-spherical or very large. We have numerically investigated whether grey dust can be emitted from high redshift galaxies without also emitting standard, reddening dust, which would have been visible in the spectra of high redshift objects. Our finding is that grain velocities are almost independent of ellipticity so that if greyness are due to the grains being elongated, it will not be possible to separate grey dust from ordinary dust. We also find that velocities are fairly independent of grain size, but we cannot rule out possible sputtering of small grains, so that large, grey dust grains could be preferentially emitted. Therefore, our conclusion is that grey dust is an unlikely explanation of the data, but we cannot rule it out if the grey dust consists of large, spherical grains.

Key words: ISM: dust, extinction – Galaxies: intergalactic medium – Cosmology: dark matter

1. Introduction

In recent years the prospect of using type Ia supernovae for distance measurements in the universe has attracted a great deal of attention. Many studies indicate that these supernovae are very close to being standard candles, so that measuring their effective magnitude amounts to directly estimating their luminosity distance. Two large scale surveys of high redshift supernovae are currently in progress (Perlmutter et al. 1998, 1997; Garnavich et al. 1998; Riess et al. 1998; Schmidt et al. 1998), and both groups have published results for the determination of the deceleration parameter, q_0. Surprisingly, the results are statistically incompatible with the value $q_0 = 1/2$ expected in the standard, flat matter dominated Friedmann model (Kolb & Turner 1990). The observed high redshift supernovae are significantly fainter than expected for $q_0 = 1/2$. Rather they are compatible with a medium density, flat universe, where roughly 70% of the energy density comes from vacuum energy (Perlmutter et al. 1998)

If this turns out to be true it is an astonishing result because it means that, taken together with the recent results on neutrino masses from Super-Kamiokande (Fukuda et al. 1998), there are at least four components contributing almost equally to the cosmic energy density budget: baryons, neutrinos, cold dark matter and vacuum energy. Even without vacuum energy this is a remarkable fine tuning, but including vacuum energy as a fourth component makes the conceptual problem substantially worse.

For this reason it is important to check all alternative explanations of the supernova data that can be thought of. One such possibility is evolution effects in the supernova progenitors. However, the data seem to indicate that the supernova population at high redshift is remarkably similar to the one known at low redshift (Perlmutter et al. 1998; Höflich, Wheeler & Thielemann 1998). Another intriguing possibility which has been advocated by Aguirre (Aguirre 1999a, 1999b) is that there could be unseen dust contamination in the data. In the data reduction it has been assumed that any possible dust follows the standard extinction law known to govern dust in the Milky Way (Cardelli, Clayton & Mathis 1989).

Based on this, almost no dust is found in the line of sight to any of the supernovae. However, this conclusion is based on the fact that dust in the Milky Way reddens significantly, simply because it is primarily made up of small, spherical grains (Draine & Lee 1984; Aguirre 1999b). This need not be the case. If there is some population of very large and/or elongated dust grains which is homogeneously distributed in the universe, this would remain undetected in reddening surveys because of its very flat extinction curve (Aguirre 1999a, 1999b), i.e. it would be "grey" dust. In fact the idea of grey dust is quite old and has been advocated as a means of thermalising the cosmic microwave background radiation in the steady state cosmology (see for instance Peebles 1993 for a review).

The above scenario could perhaps be a viable explanation of the data, given that enough such dust can be expelled from galaxies at high redshift *without* simultaneously expelling small dust grains.

The purpose of the present paper is to quantify this by numerical modelling of dust expulsion. We have wished to investigate whether it is in fact possible to expel only very elliptical and large grains. We have not worried about the possible production mechanisms for dust grains, only about their dynamical behaviour. A completely different problem is whether it is at all possible to produce the required amounts of large dust grains in the first place. However, by using our relatively simple model we are able to make the very robust prediction that dust segregation at the level needed to explain the data is not possible, unless very special conditions prevail in the host galaxies. Note that in the present paper we only consider radiation pressure as a source of dust expulsion. There could be several other ways of removing dust from galaxies, such as winds from supernovae (Suchkov et al. 1994) or galaxy collisions (see e.g. Gnedin 1998). However, these methods seem unlikely to preferentially emit large dust grains, and for that reason we have, in accordance with Aguirre (1999a, 1999b) concentrated on radiation pressure, even though galaxy collisions might be the most efficient method of dust removal at high redshift (Gnedin 1998).

The paper has been sectioned as follows: Section 2 contains a discussion of the equation of motion for dust grains in a galactic environment, section 3 contains our main numerical results, and finally section 4 is devoted to a discussion of our findings.

2. Equation of motion for dust grains in a galactic medium

At present the supernovae with the highest measured redshifts are at $z \simeq 0.8$ (Perlmutter et al. 1998). This means that if dust is to explain the data it must be expelled and distributed uniformly prior to this epoch. For this to happen it must have been expelled from the host galaxies at very high redshift, probably $z \simeq 3$ or more (Aguirre 1999a, 1999b). Relatively little is known about the structure of galaxies at such distances, except that they are richer in gas content than our own galaxy at present.

We have taken a heuristic approach to our lack of knowledge about the nature of the host galaxies and calculated dust expulsion for a range of different gas contents and emission temperatures. We find that our results depend very little on these assumptions.

We assume that a given spiral galaxy can be reasonably well approximated by three components: disk, bulge and halo. The disk is taken to be an infinitely thin axially symmetric exponential distribution of matter. The bulge, which is massive and luminous, is just added to the center of the galactic disk, and the halo is a spherical symmetric mass structure considered to be completely dark.

The three main contributions to the force acting on a dust grain moving through a galaxy are gravity, radiative forces and drag forces. As the galaxy is assumed to be axially symmetric, all calculations are done in cylindrical coordinates (R, z, ϕ).

In the following we shall always work with ellipsoidal dust grains, with semiaxes a and b. The effective radius of such a grain is then defined by the relation

$$V \equiv \frac{4}{3}\pi a_{\rm eff}^3 = \frac{4}{3}\pi a^2 b. \tag{1}$$

2.1. Gravitational forces

The gravitational force on a dust grain of mass $m_{\rm g} \equiv \rho_g V$, where ρ_g is the grain density, is simply given by

$$\mathbf{F}_{\rm G} = m_{\rm g}\mathbf{G}(\mathbf{r}), \tag{2}$$

where $\mathbf{G}(\mathbf{r})$ is the gravitational field intensity at the point $\mathbf{r}$.

The disk has an exponential mass distribution with surface density

$$\Sigma(R) = \Sigma_0 \exp(-R/R_{\rm d}), \tag{3}$$

where $R_{\rm d}$ is the disk scale length. The potential generated by this disk is most easily expressed via Bessel functions, and takes the form (see e.g. Binney & Tremaine 1987)

$$\Phi(R,z) = -2\pi G\Sigma_0 R_{\rm d}^2 \int_0^\infty \frac{J_0(kR)\exp(-kz)}{[1+(kR_{\rm d})^2]^{3/2}}{\rm d}k, \tag{4}$$

$J_n(x)$ being the Bessel function of the first kind of order n. The gravitational force from the disk on a dust grain with mass $m_{\rm g}$ is thus given by

$$\begin{aligned} F_{{\rm grav,disk},R} &= -m_{\rm g}2\pi G\Sigma_0 R_{\rm d}^2 \int_0^\infty \frac{kJ_1(kR)\exp(-kz)}{[1+(kR_{\rm d})^2]^{3/2}}{\rm d}k, \\ F_{{\rm grav,disk},z} &= -m_{\rm g}2\pi G\Sigma_0 R_{\rm d}^2 \int_0^\infty \frac{kJ_0(kR)\exp(-kz)}{[1+(kR_{\rm d})^2]^{3/2}}{\rm d}k. \end{aligned} \tag{5}$$

The potential from the bulge is that of a point mass with mass $M_{\rm b}$. That is,

$$F_{{\rm grav,bulge},r} = -\frac{GM_{\rm b}m_{\rm g}}{r^2}, \tag{6}$$

where $r = \sqrt{R^2+z^2}$. Projecting on to the R and z axis gives

$$\begin{aligned} F_{{\rm grav,bulge},R} &= -\frac{GM_{\rm b}m_{\rm g}}{r^2}\frac{R}{r} = -GM_{\rm b}m_{\rm g}\frac{R}{(R^2+z^2)^{3/2}}. \\ F_{{\rm grav,bulge},z} &= -\frac{GM_{\rm b}m_{\rm g}}{r^2}\frac{z}{r} = -GM_{\rm b}m_{\rm g}\frac{z}{(R^2+z^2)^{3/2}}. \end{aligned} \tag{7}$$

For the halo we assume an isothermal sphere distribution

$$\rho = \rho_0 \frac{a_h^2}{a_h^2 + r^2}. \tag{8}$$

Integrating the equation for ρ yields

$$M(r) = 4\pi\rho_0 a_{\rm h}^2[r - a_{\rm h}\arctan(r/a_{\rm h})], \quad (9)$$

where ρ_0 is the central density and $a_{\rm h}$ is the halo mass scale length. Setting $M_{\rm h} = M(r)$, this results in a central force, which after projecting on to the R and z axis takes the form

$$F_{{\rm grav,halo},R} = -GM_{\rm h}m_{\rm g}\frac{R}{(R^2+z^2)^{3/2}},$$
$$F_{{\rm grav,halo},z} = -GM_{\rm h}m_{\rm g}\frac{z}{(R^2+z^2)^{3/2}}. \quad (10)$$

2.2. Radiative forces

The radiation pressure force can be written in a way completely analogous to the gravitational force (Ferrara et al. 1991).

First, we shall assume that the spectral function, Ω_ν, of the emitted light is constant throughout the galaxy, i.e.

$$\Omega_\nu(R,z) = \Omega_\nu. \quad (11)$$

If this is the case then we can calculate a spectrally averaged radiation pressure coefficient for a given dust grain as

$$Q^*_{\rm pr} = \int d\nu \Omega_\nu Q_{\rm pr}(\nu), \quad (12)$$

which applies at all positions in the galaxy. In practise we shall assume that the galaxy emits light as a black body with some temperature T_0, so that $\Omega_\nu = B_\nu(T_0)$, where B_ν is the Planck function, and $Q^*_{\rm pr}(a_{\rm eff}) = Q_{\rm pr}(a_{\rm eff}, T_0)$.

The disk luminosity distribution is assumed exponential like the mass distribution, and with the same scale length $R_{\rm d}$

$$I(R) = I_0\exp(-R/R_{\rm d}). \quad (13)$$

From these simple assumptions the radiation pressure force from the disk is given as

$$F_{{\rm rad,disk},R} = \frac{2\pi^2 a_{\rm eff}^2 Q^*_{\rm pr} I_0}{c}\int_0^\infty \frac{kJ_1(kR)\exp(-kz)}{[1+(kR_{\rm d})^2]^{3/2}}{\rm d}k,$$
$$F_{{\rm rad,disk},z} = \frac{2\pi^2 a_{\rm eff}^2 Q^*_{\rm pr} I_0}{c}\int_0^\infty \frac{kJ_0(kR)\exp(-kz)}{[1+(kR_{\rm d})^2]^{3/2}}{\rm d}k, \quad (14)$$

analogous of Eq. (5).

The force from the bulge is similarly given as

$$F_{{\rm rad,bulge},r} = \frac{\pi a_{\rm eff}^2 Q^*_{\rm pr}}{c}\frac{L_b}{4\pi r^2}, \quad (15)$$

where L_b is the total luminosity of the bulge. In the R and z directions this is

$$F_{{\rm rad,bulge},R} = \frac{a_{\rm eff}^2 Q^*_{\rm pr} L_{\rm b}}{4c}\frac{R}{(R^2+z^2)^{3/2}},$$
$$F_{{\rm rad,bulge},z} = \frac{a_{\rm eff}^2 Q^*_{\rm pr} L_{\rm b}}{4c}\frac{z}{(R^2+z^2)^{3/2}}, \quad (16)$$

again, apart from numerical factors equal to Eq. (7).

Note that there is an important issue which we do not address here, namely the opacity in the disk itself (Davies et al. 1998). Since the disk contains significant amounts of dust it will obscure the starlight and lead to smaller radiation pressure. This was determined to be an important effect for the dynamical evolution of grains by Davies et al. (1998).

However, it is not entirely clear how disk opacity affects the grain evolution. It leads to smaller radiation pressure, but on the other hand it also reddens the light, leading to a lower effective temperature of the radiation field. We model this behaviour by calculating grain evolution for several different emission temperatures.

2.3. Rotation

The stars and gas in the disk of spiral galaxies have purely rotational orbits. This means that the rotational velocity is given by

$$v_{\rm rot} = \sqrt{R\frac{\partial\Phi}{\partial R}}. \quad (17)$$

Initially the grain also rotates with this velocity, but as the grain moves outwards the rotational velocity decreases. If gas drag is neglected the angular momentum in the z direction is conserved so that

$$v_{\rm rot}(R) = v_{\rm rot}(R_i)(R_i/R). \quad (18)$$

However, for typical spiral galaxies the rotational velocity of the stars remains constant out to very large values of R. This means that grains will, in general, be spun up by interaction with the disk gas. This effect is in practice quite small, but we have included it anyway.

2.4. Drag forces

The interaction of dust grains with gas plays an important role in grain evolution. Assuming that the grain moves fast compared with the thermal velocities in the gas, the exact expression for the drag force experienced by a grain is (Il'in 1994)

$$\mathbf{F}_{\rm drag} = -\pi ab\rho_{\rm gas}v_{\rm g}^2\frac{2}{\pi}E([1-e^2]\sin^2\Theta)\hat{\mathbf{v}}_{\rm g} \quad (19)$$

where a and b are the semiaxes of the spheroidal grain, $e = a/b$, $\mathbf{v}_{\rm g}$ the grain velocity relative to the gas, $E(x)$ the complete elliptic integral of the second kind and Θ the angle between magnetic field direction and wave vector of radiation.

Interstellar dust grains rotate with large angular velocity because of the angular momentum transferred to them by collisions. Non-spherical grains are likely to rotate along the axis of maximum moment of inertia, with the angular momentum being aligned along the magnetic

field lines (Il'in 1994). For this reason Θ is likely to be small so that the argument to the elliptic integral is close to 0. Since $E(0) = \pi/2$ the drag force becomes

$$\mathbf{F}_{\rm drag} = -\pi ab\rho_{\rm gas} v_{\rm g}^2 \hat{\mathbf{v}}_{\rm g}. \quad (20)$$

As mentioned above, this drag force also causes the grain to be spun up by the gas, so that, as long as it stays in the gas, $\mathbf{v}_\phi$, is driven towards the rotational velocity of the gas. Note that $[1-e^2]\sin^2\Theta \in [0,1]$ so that $E(x) \in [1, \pi/2]$ always, i.e. choosing $x = 0$ produces at worst an error of 50% in the drag force.

Also, the above formula only applies if the grain velocity is larger than the thermal velocity of the gas. However, using Eq.(19) leads to small errors, as will be discussed in section 3.1.

2.5. Sputtering

In general, grains are eroded as they pass through the galactic medium, by collisions with gas particles and by radiation (Draine & Salpeter 1979, Ferrara et al. 1991, Shustov & Vibe 1995). The amount of sputtering increases with gas density, both because of the higher collision rate and because the grain spends more time in the region with high gas density. The effect of sputtering is primarily to destroy very small dust grains, but leave large dust grains more or less unscathed (Ferrara et al. 1991, Davies et al. 1998). It is very difficult to assess the amount of sputtering in a given galaxy. For galaxies similar to the Milky Way, Ferrara et al. (1991) find that sputtering is not important unless the grains are very small ($a \sim 10-20$ nm), whereas Shustov & Vibe (1995) find that grains up to 50 nm could be destroyed. We can therefore not rule out possible destruction of grains up to about this size.

2.6. Magnetic forces

As has been noted many times in the literature, galactic magnetic fields are important for the dynamical evolution of dust. However, very little is known about the nature of these fields, so we have chosen to neglect possible magnetic fields in the present study. In general, the effect of the magnetic field will be to enhance the confinement of grains because the drag force on grains is enhanced (Ferrara et al. 1991) and because they are forced to move along the field lines (Ferrara et al. 1991; Davies et al. 1998).

3. Numerical results

In order to do actual numerical calculations it is necessary to specify relevant parameters for the host galaxy. In practice we have taken the present day Milky Way with parameters as specified in Table 1 (Binney & Tremaine 1987, Ferrara et al. 1991). This may not be a very accurate description of a typical high redshift galaxy, but as will be shown the numerical results are fairly insensitive to these assumptions. The most important issues are the emission temperature of the galaxy and the amount of gas contributing to the drag force. We have modelled the radiation field of the galaxy as a black body with temperature, $T_0 = 6000$ K, 9000 K or 12000 K.

Table 1. Physical parameters for our sample galaxy (the Milky Way).

	Parameter	value
Disk	Σ_0	381.9 $M_\odot$ pc^{-2}
	R_d	5 kpc
	I_0	108.28 $L_\odot$ pc^{-2}
Bulge	M_b	1.0×10^{10} $M_\odot$
	L_b	1.5×10^9 $L_\odot$
Halo	ρ_0	6.3×10^{-24} g cm^{-3}
	a_h	2.8 kpc

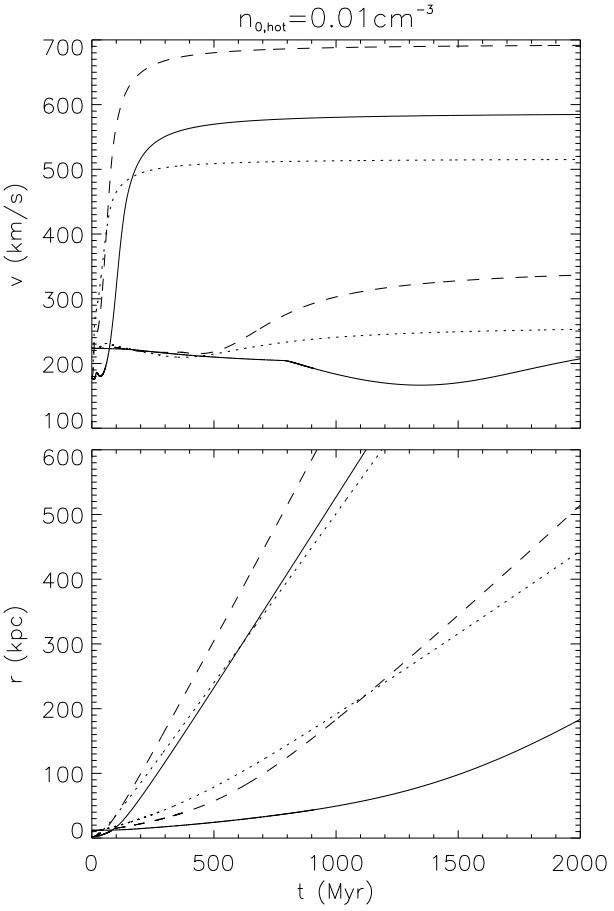

Fig. 1. Grain velocity v and displacement r for the present day Milky Way model, with $(a_{\rm eff}, e) = (50\,{\rm nm}, 1), (50\,{\rm nm}, 1/8), (300\,{\rm nm}, 1)$ (full, dashed and dotted curves respectively), and initial galactocentric distance $R_0 = 2\,{\rm kpc}$ (upper three curves) and $R_0 = 12\,{\rm kpc}$ (lower three curves). Notice that the initial velocity is due to rotation.

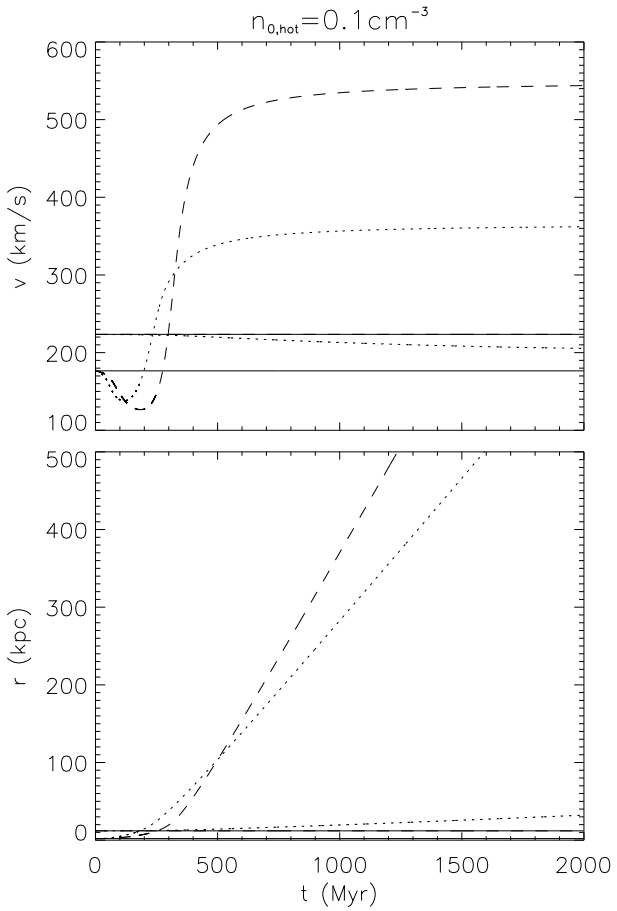

Fig. 2. Grain velocity v and displacement r for our extremely gas rich model, with $(a_{\rm eff}, e) = (50\,{\rm nm}, 1), (50\,{\rm nm}, 1/8), (300\,{\rm nm}, 1)$ (full, dashed and dotted curves respectively), and initial galactocentric distance $R_0 = 2\,{\rm kpc}$ (lowest initial v) and $R_0 = 12\,{\rm kpc}$ (highest initial v). Notice that two of the $R_0 = 12\,{\rm kpc}$ curves overlap, and that the initial velocity is due to rotation.

Furthermore we have considered three different models for the gas distribution. In all three cases we model the gas by two different components, a cold gas and a hot halo gas. Both components are assumed to have the number density distribution

$$n(R, z) = n_0 e^{-z/z_s}, \tag{21}$$

i.e. constant density as a function of R and an exponential fall-off with z. The cold component is assumed to have $z_s = 170$ pc, and the hot $z_s = 2$ kpc. For the three different models we then use the following values for n_0

1: $n_{0,\rm hot} = 1.0 \times 10^{-4}\,{\rm cm}^{-3}$, $n_{0,\rm cold} = 2.0 \times 10^{-3}\,{\rm cm}^{-3}$
2: $n_{0,\rm hot} = 1.0 \times 10^{-2}\,{\rm cm}^{-3}$, $n_{0,\rm cold} = 2.0 \times 10^{-1}\,{\rm cm}^{-3}$
3: $n_{0,\rm hot} = 1.0 \times 10^{-1}\,{\rm cm}^{-3}$, $n_{0,\rm cold} = 2.0\,{\rm cm}^{-3}$

The first model corresponds to the extreme case of an almost empty galaxy, the second roughly to the present day Milky Way (Lockman 1991; Heiles 1991), and the third to an extremely gas enriched galaxy. In all cases we assume that gas is made entirely of hydrogen. Note that we have assumed a model with constant density as a function of R. This may seem a strong assumption, but as will be shown in the next section the numerical results depend relatively little on it.

The next important issue is the physical composition of the dust grains. Aguirre 1999a assumed pure graphite grains, but relaxed that assumption in a subsequent study (Aguirre 1999b), where a more realistic galactic dust composition of silicate and graphite was assumed.

Again, we have taken an heuristic approach and calculated our models for two different cases, amorphous carbon and graphite-like carbon; silicates are expected to behave very similarly. To find the radiation pressure coefficient for these grains we have used dielectric data from Jäger et al. 1998. They have obtained dielectric data on carbon pyrolised in the laboratory at different temperatures. Their 400 C sample has an amorphous structure while their 1000 C sample closely resembles graphite. Both are bulk samples and therefore isotropic. Note that the graphite needles used in the Aguirre (1999a) model are highly anisotropic, i.e. they are macrocrystals, whereas our data comes from a bulk sample containing microcrystals. However, in practice the difference between these two assumptions is likely to be small, so that our results apply to the Aguirre (1999a) scenario. We take these two samples as extreme cases of carbon composition in dust grains. Using this data we have proceeded to calculate the radiation pressure coefficient by use of the Discrete Dipole approximation as implemented in the DDSCAT package (Draine & Flatau 1998). The resulting $Q^*_{\rm pr}$ are tabulated in A.

Next, we have performed the full numerical solution to the dynamical equations for ellipsoidal grains of different ellipticities and sizes. Specifically we have calculated for $a_{\rm eff} = 25, 50, 100, 150, 200, 250, 300\,{\rm nm}$, and $e = 1, 1/2, 1/4, 1/8, 1/16$ for each $a_{\rm eff}$. The calculations have been done for twelve different initial values of R, equally spaced from 1-12 kpc, and always starting at $z = 0.2$ kpc. The grains were followed for a period of 2 Gyr to determine their final velocity. Figs. 1 and 2 show some examples of velocities and displacements $r = (R^2 + z^2)^{1/2}$ as a function of time, for the present day Milky Way and for our extremely gas enriched model. In each case the velocity and displacement are shown for three combinations of $a_{\rm eff}$ and e, namely $(a_{\rm eff}, e) = (50\,{\rm nm}, 1), (50\,{\rm nm}, 1/8), (300\,{\rm nm}, 1)$, and for two different initial galactocentric distances $R_0 = 2, 12\,{\rm kpc}$. We have used Q values for the appropriate size and shape at $T_0 = 9000\,{\rm K}$. Both figures show that it is quite difficult to expel dust which has a large initial galactocentric distance, whereas most dust is expelled rapidly from the galactic center. In the gas rich model, we find that grains starting at $R = 12$ kpc are almost completely

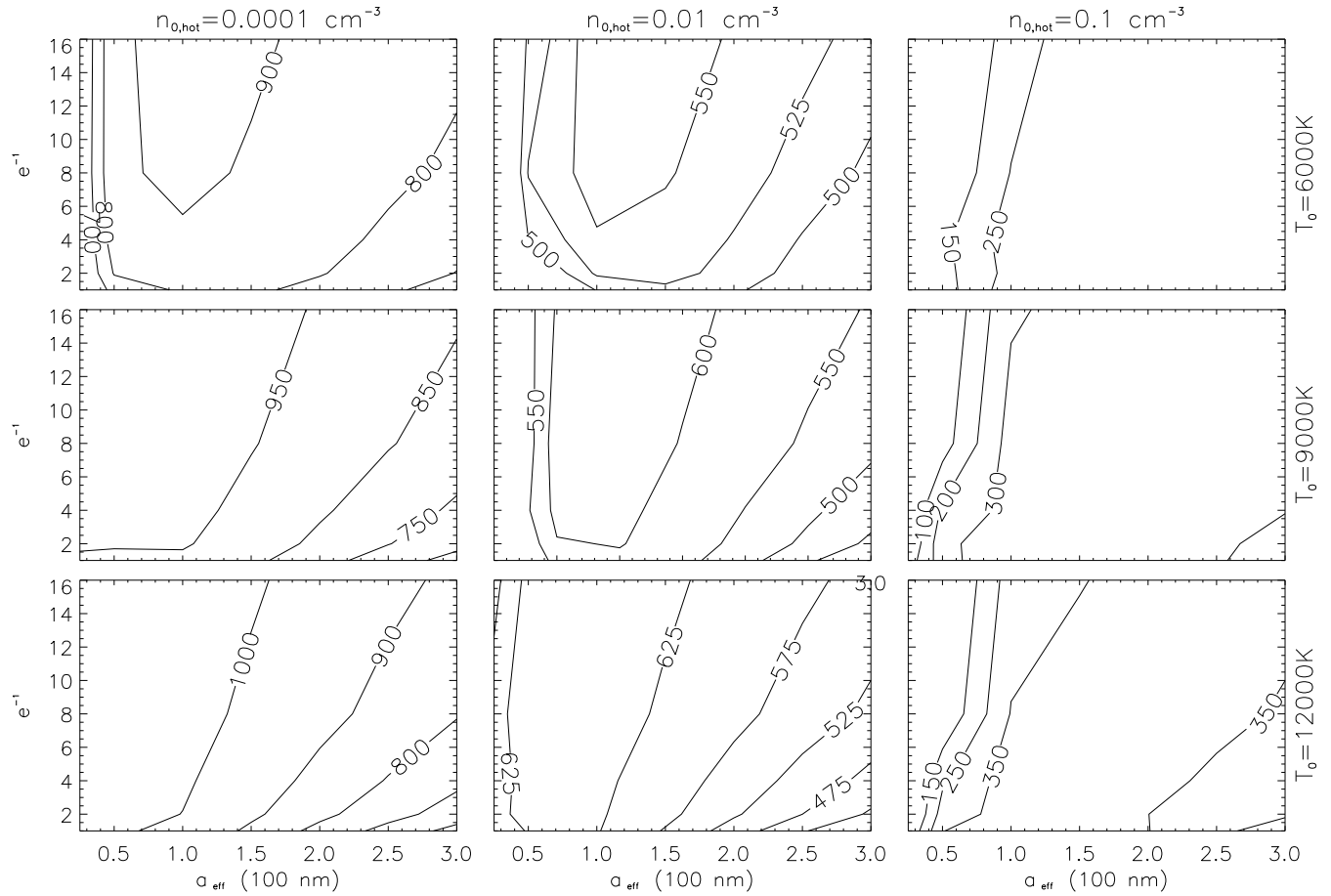

Fig. 3. Contours of constant velocity in the $(a_{\rm eff}, e^{-1})$ plane for graphite like carbon grains (1000 C sample from Jäger et al. 1998).

confined by drag forces. The figures also show that grains of different sizes and ellipticities behave fairly similarly.

After solving the dynamical equations, we have then calculated the final velocity of the dust grains, averaged over the entire galaxy. To do this we have assumed that the dust production rate is proportional to the light profile of the disk, i.e. $R \propto e^{-R/R_d}$. In some cases dust grains are confined within the galaxy by drag forces in the gas. This happens particularly in the outer parts of the host galaxy and in the gas rich model. For such grains we set the final velocity equal to zero. This means that our averaged velocity is in fact an average over *all* grains, not only the ones which escape. Thus, the averaged final velocities are in fact a folding of the velocity of escaping dust grains and escape probabilities.

Figs. 3 and 4 summarise our results for graphite and amorphous carbon respectively, showing contours of constant velocity in the $(a_{\rm eff}, e^{-1})$ plane, for all combinations of base density n_0 (represented by $n_{0,\rm hot}$ on top of the columns) and temperature T_0 (to the right of each row). Exactly as expected the averaged velocity is a decreasing function of the gas density and an increasing function of emission temperature (unless the grains are very large).

Our main result is that the final grain velocity is a very slowly varying function of ellipticity. The reason is that although the effective Q-value increases with ellipticity if the effective radius is kept fixed, the drag force increases too. Drag therefore acts as a "velocity-moderator" in the sense that it tends to erase velocity difference due to ellipticity.

The differences in final velocity due to varying grain size is straightforward to understand. The acceleration due to radiation pressure is proportional to $a_{\rm eff}^{-1}$ so that one should expect decreasing final velocities for larger grains. However, the effective Q-value is a strongly increasing function of $a_{\rm eff}$ for small grains (up to roughly 100 nm), so that in the end there will be some $a_{\rm eff}$ where the velocity peaks. Exactly this effect is seen in Figs. 3 and 4.

Note that in the upper left plot of fig. 4 the velocity increases again at very small radii. This is probably a numerical artifact produced by uncertainty in the calculation of the effective Q-value by the program DDSCAT. A few test runs have shown that increasing the number

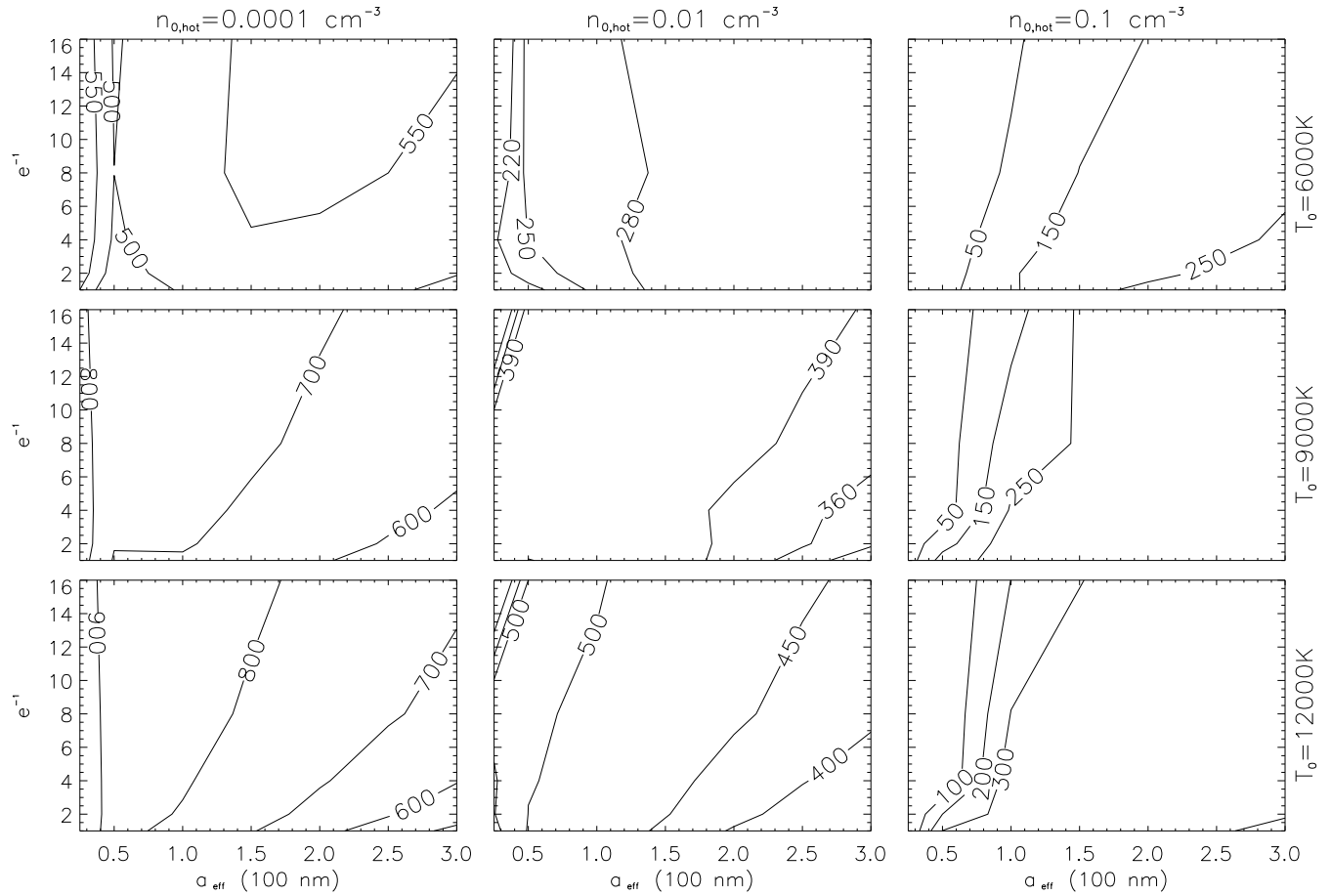

Fig. 4. Contours of constant velocity in the $(a_{\rm eff}, e^{-1})$ plane for amorphous carbon dust grains (400 C sample from Jäger et al. 1998).

of discrete dipoles in the grain does diminish the Q value, but at much incresed computational time.

Our numerical results thus indicate that it will be difficult to separate dust grains of different ellipticities, but that in certain cercumstances it could be possible to expel large grains only.

3.1. Model dependencies

We have investigated how dependent our conclusions are on our assumptions about the drag force and the number density distribution of the gas, by performing some sample calculations using more conservative assumptions.

In calculating the drag force, the grain velocities were assumed to be large compared to the thermal velocities in the gas. But adopting gas temperatures of 100K and 10^6K for the cold and hot gas component respectively, the average thermal velocity of the hot component is $v_{\rm gas} \simeq 130$km/s, which is not negligible compared to the smaller grain velocities. In order to check the validity of using our Eq. (19) we recalculated the final averaged velocities of amorphous carbon grains in the model with base densities representative of the present day Milky Way (the second model), using the approximate formula for the drag force given by Il'in (1994, Eq. 23). This approximation is designed to be valid for all grain velocities. The results are shown in the first column of figure 5.

Even though our equation can produce errors of roughly 25% in absolute velocities, it has no effect on the conclusion that grain velocities are fairly independent of size and ellipticity.

For the gas we assumed that the number density distribution was constant as a function of R. We have investigated the effect of this by performing a calculation using an exponential fall-off with both R and z. We use base densities of $n_{0,\rm cold} = 1.1\,{\rm cm}^{-3}$ and $n_{0,\rm hot} = 0.05\,{\rm cm}^{-3}$, and the same scale length as the stellar disk. This produces densities equal to those of the present day Milky Way at $R_0 \sim 8.5\,$kpc. Here we return to using the expression for the drag force given by Eq. (19). The results are shown in the second column of figure 5. Again, this yields results which are somewhat different in absolute magni-

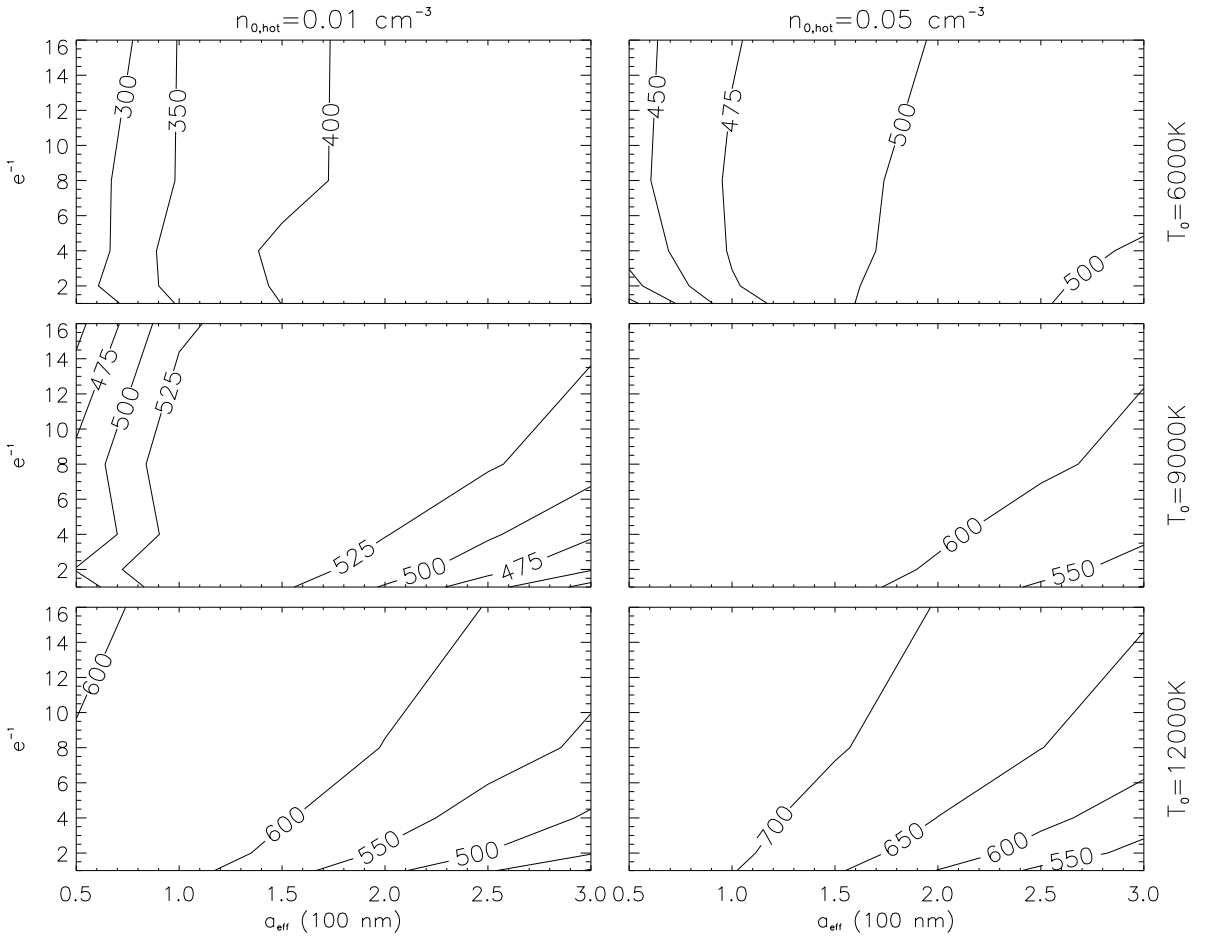

Fig. 5. Contours of constant velocity in the $(a_{\rm eff}, e^{-1})$ plane for amorphous carbon dust grains using the approximate drag force from Il'in (1994) (left column), and with exponential fall-off in number density with R (right column).

tude relative to those found from the constant density gas disk. However, the velocity differences due to different size and ellipticity are still small, which is the main point.

In light of the large uncertanties in these calculations, because of our poor knowledge of the nature of high-redshift galaxies, we think our approximations are reasonable. They do yield different absolute results, but have no bearing on our conclusion about the relative velocities of different dust grains.

4. Discussion

We have performed numerical calculations of how dust grains are expelled from galaxies by the radiation pressure produced by starlight. The calculations were done for a whole range of different sizes and shapes, as well as for several different host galaxy types. In all cases, final grain velocities are almost independent of ellipticity. Our conclusion therefore is that the original scenario of Aguirre (1999a) does not work.

Also, if the galaxy does not contain significantly more gas than the present day Milky Way, the relative velocity difference between grains of different sizes is quite small, unless the grains become small.

The mechanism proposed by Aguirre (1999b) requires that only dust with effective radius larger than about 100 nm should escape to the intergalactic medium, in order not to have excessive reddening (this can be relaxed to about 50 nm if only graphite grains are considered (Aguirre 1999b)). Our results indicate that this mechanism does not work for the two models with the least gas content (the first two columns in Figs. 3 and 4), unless the smaller grains are destroyed completely by sputtering. However, the findings of Ferrara et al. (1991) and Davies et al. (1998), indicate that sputtering is not effective unless the radius becomes as low as 10 nm. On the other hand, Shustov & Vibe (1995) find that grains up to 50 nm can be destroyed. In light of our poor understanding of the sputtering mechanism it is not possible to rule out the Aguirre model. However, just from looking at grain velocities the model does seem an unlikely explanation.

As for the third model with extremely large gas content, there is a difference between small and large grains, the smaller grains having lower velocities. This seems to be exactly the type of selection effect we are looking for and, furthermore, the model where it happens could be quite similar to high redshift galaxies. However, the result should be treated with caution because this model is already close to the limit where all grains are completely confined by gas drag. Altogether we find that there *are* models where dust segregation can be produced, but that the physical conditions have to be just right. We can therefore not rule out the Aguirre (1999b) model, only say that it requires some fine tuning.

Our results indicate that most of the dust produced in galaxies will be expelled by radiation pressure. Of course we have neglected galactic sputtering of grains, which might destroy very small grains. However, measurements indicate that the intergalactic medium in fact has a fairly high metal content (Mushotsky 1996). This in turn is likely to mean that most of the produced dust is expelled from the host galaxies. However, it also seems very likely that almost all of the dust is subsequently destroyed in the intracluster medium (Dwek et al. 1990, Stickel et al. 1998). Note that since there is probably effective sputtering in the intracluster medium, this could also mean that selection of large dust grains could be due to sputtering in the ICM. This also limits our ability to rule out the Aguirre (1999b) scenario. We can only say that sputtering within galaxies is an unlikely explanation.

The above discussion does not take into account that radiation pressure may not even be a dominant mechanism for dust expulsion at high redshift. As mentioned above, Gnedin (1998) has argued that galaxy mergers may provide the most efficient mechanism for expulsion of grains into the intergalactic medium. If this is the case there is even less reason for suspecting that grains with flat opacity curves should preferentially be emitted, and the above scenario will be even less credible.

Note added – After this paper had been submitted there has been a growing interest in the possibility of progenitor evolution systematically biasing the SNIa data. At present it seems unclear what the effects of evolution are, but it has been pointed out that if there is evolution, then it will be very difficult to extract cosmological parameters from the data (Drell, Loredo & Wasserman 1999; Dominguez et al. 1999; Riess et al. 1999; Wang 1999).

Acknowledgements. We wish to thank Anja C. Andersen for many enlightening conversations regarding the properties of interstellar dust grains. Also, we wish to thank the anonymous referee for many constructive and enlightening comments on the initial version of this paper.

Appendix A: Radiation pressure coefficients

The following table shows the averaged radiation pressure coefficients $Q^*_{\rm pr}$ as a function of $a_{\rm eff}$, e and radiation field temperature T_0, calculated for amorphous carbon and graphite. $a_{\rm eff}$ is in units of 100nm.

Table A.1. Effective radiation pressure coefficients, $Q^*_{\rm pr}$, for different grain sizes and ellipticities.

Carbon, $T_0 = 6000\,$K					
$a_{\rm eff}\backslash e$	1	1/2	1/4	1/8	1/16
0.25	0.15	0.17	0.18	0.19	0.20
0.5	0.33	0.36	0.38	0.39	0.40
1.0	0.74	0.78	0.80	0.82	0.83
1.5	1.15	1.19	1.21	1.24	1.25
2.0	1.52	1.56	1.60	1.64	1.66
2.5	1.82	1.88	1.94	2.01	2.06
3.0	2.05	2.15	2.25	2.36	2.43
Carbon, $T_0 = 9000\,$K					
0.25	0.27	0.29	0.30	0.31	0.32
0.5	0.56	0.59	0.61	0.63	0.63
1.0	1.09	1.13	1.17	1.21	1.23
1.5	1.52	1.58	1.64	1.71	1.78
2.0	1.82	1.92	2.03	2.16	2.27
2.5	2.01	2.18	2.34	2.54	2.70
3.0	2.11	2.36	2.59	2.86	3.09
Carbon, $T_0 = 12000\,$K					
0.25	0.37	0.39	0.40	0.40	0.41
0.5	0.72	0.75	0.77	0.79	0.80
1.0	1.29	1.34	1.39	1.46	1.51
1.5	1.67	1.77	1.87	2.01	2.12
2.0	1.88	2.07	2.24	2.45	2.63
2.5	1.99	2.26	2.50	2.81	3.07
3.0	2.01	2.37	2.69	3.09	3.43
Graphite, $T_0 = 6000\,$K.					
0.25	0.26	0.31	0.35	0.39	0.40
0.5	0.57	0.65	0.73	0.79	0.82
1.0	1.26	1.38	1.48	1.56	1.61
1.5	1.87	1.99	2.09	2.20	2.30
2.0	2.30	2.45	2.57	2.73	2.89
2.5	2.56	2.76	2.93	3.16	3.29
3.0	2.69	2.95	3.18	3.51	3.82
Graphite, $T_0 = 9000\,$K.					
0.25	0.38	0.42	0.45	0.48	0.49
0.5	0.79	0.86	0.92	0.96	0.98
1.0	1.56	1.64	1.71	1.79	1.86
1.5	2.07	2.20	2.31	2.45	2.59
2.0	2.35	2.55	2.73	2.98	3.20
2.5	2.47	2.76	3.02	3.37	3.70
3.0	2.48	2.85	3.19	3.67	4.10
Graphite, $T_0 = 12000\,$K.					
0.25	0.45	0.49	0.51	0.53	0.54
0.5	0.92	0.97	1.01	1.04	1.06
1.0	1.69	1.75	1.81	1.90	1.98
1.5	2.10	2.27	2.40	2.57	2.72
2.0	2.28	2.54	2.78	3.10	3.34
2.5	2.31	2.67	2.99	3.45	3.85
3.0	2.25	2.70	3.12	3.68	4.22

References

Aguirre, A.N., 1999a, Astrophys. J. Lett. 512, L19.

Aguirre, A.N., 1999b, astro-ph/9904319.

Barsella, B. et al., 1989, A&A, 209, 349.

Binney, J. & Tremaine, S., 1987, Galactic Dynamics, J.P. Ostriker (ed.), Princeton.

Cardelli, J.A., Clayton, C.G., and Mathis, J.S., 1989, Astrophys. J. 345, 245.

Davies, J.I. et al., 1998, MNRAS, 300, 1006.

Dominguez, I. et al., 1999, astro-ph/9905047.

Draine, B.T. & Flatau, P.J., 1998, Princeton observatory preprint POPe-785.

Draine, B.T. & Lee, H., 1984, Astrophys. J., 285, 89.

Draine, B.T. & Salpeter, E.E., 1979, Astrophys. J., 231, 77.

Drell, P.S., Loredo, T.J. & Wasserman, I., 1999, astro-ph/9904111.

Dwek, E., Rephaeli, Y. & Mather, J.C., 1990, Astrophys. J. 350, 104.

Ferrare, A. et al., 1991, Astrophys. J., 381, 137.

Fukuda, Y. et al., 1998, Phys. Rev. Lett. 81, 1562.

Garnavich, P.M. et al., 1998, astro-ph/9806396 (to appear in Astrophys. J.).

Gnedin, N.Y., 1998, MNRAS, 294, 407.

Heiles, C., 1991, *The Interstellar Disk-Halo Connection in Galaxies*, proceedings of the 144th symposium of the IAU, Leiden 1990, Kluwer Academic Publishers.

Höflich, P., Wheeler, J.C., and Thielemann, F.K., 1998, Astrophys. J., 495, 617 (1998).

Il'in, V.B., 1994, A&A, 281, 486.

Jäger, C., Mutschke, H. & Henning, T., 1998, A&A, 332, 291-299.

Kolb, E.W. & Turner, M.S., 1990, *The Early Universe*, Addison-Wesley Press.

Lockman, F.J., 1991, *The Interstellar Disk-Halo Connection in Galaxies*, proceedings of the 144th symposium of the IAU, Leiden 1990, Kluwer Academic Publishers.

Mushotsky, R. et al., 1996, Astrophys. J. 466, 686.

Peebles, P.J.E., 1993, *Principles of Physical Cosmology*, Princeton University Press.

Perlmutter, S. et al., 1997, Astrophys. J. 483, 565.

Perlmutter, S. et al., 1998, astro-ph/9812133 (to appear in Astrophys. J.).

Riess, A.G. et al., 1998, astro-ph/9805201 (to appear in Astron. J.).

Riess, A. G. et al., 1999, astro-ph/9907038.

Schmidt, B.P. et al., 1998, astro-ph/9805200 (to appear in Astrophys. J.).

Shustov, B.M. & Vibe, D.Z., 1995, Astron. Zhurnal, 72, 650.

Stickel, M. et al., 1998, A&A, 329, 55.

Suchkov, A. et al., 1994, Astrophys. J. 430, 511.

Wang, Y., 1999, astro-ph/9907405.